IEEE Access
Multidisciplinary | Rapid Review | Open Access Journal

Date of publication xxxx 00, 0000, date of current version xxxx 00, 0000.

Digital Object Identifier 10.1109/ACCESS.2017.Doi Number

Artificial Neural Network and Newton Raphson (ANN-NR) algorithm based Selective Harmonic Elimination in Cascaded Multilevel Inverter for PV Applications

P. Sanjeevikumar[1], Senior Member, IEEE, Dhanamjayulu C[2], Member, IEEE, Baseem Khan[3], Member, IEEE

[1] CTIF Global Capsule (CGC) Laboratory, Department of Business Development and Technology, Aarhus University, Birk Centerpark 15, 7400 Herning, Denmark.
[2] School of Electrical Engineering, Vellore Institute of Technology (VIT) University, Vellore, Tamilnadu, India.
[3] Department of Electrical and Computer Engineering, Hawassa University, Hawassa, Ethiopia, 05.

Corresponding author: C. Dhanamjayulu (e-mail: dhanamjayulu.c@vit.ac.in) and Baseem Khan (e-mail: baseem.khan04@gmail.com)

ABSTRACT In this article, a hybrid Artificial Neural Network - Newton Raphson (ANN-NR) is introduced to mitigate the undesired lower-order harmonic content in the cascaded H-Bridge multilevel inverter for solar photovoltaic (PV). Harmonics are extracted by the excellent choice of opting switching angles by exploiting the Selective Harmonic Elimination (SHE) PWM technique accompanying a unified algorithm in order to optimize and reduce the Total Harmonic Distortion (THD). ANN is trained with optimum switching angles, and the estimates generated by the ANN are the initial guess for NR. In this study, the CHB-MLI is combined with a traditional boost converter, it boosts the PV voltage to a superior dc-link voltage Perturb and Observe (P&O) based Maximum Power Point Tracking (MPPT) algorithm is used for getting a stable output and efficient operation of solar PV. The proposed system is proved over an eleven-level H-bridge inverter, the work is carried out in MATLAB/Simulink environment, and the respective results are confirmed that the proposed technique is efficient, and offers an actual firing angles with a few iterations results in a better capability of confronting local optima values. The suggested algorithm is justified by the experimental development of eleven-level cascaded H-bridge inverter.

INDEX TERMS Artificial Neural Network (ANN), Selective Harmonic Elimination (SHE) PWM, Newton Raphson (NR) method, Perturb & Observe (P&O), Maximum Power Point Tracking (MPPT).

I. INTRODUCTION

In the recent past, most of the modernized industries have pioneered to offer higher power devices. Certain utilities expect large-power and medium voltage levels provides more demand which consists of only one switch with the low rated power grid [1]. Simultaneously, the usage of microprocessor-controlled devices, digital, electronic sensitive equipment, and nonlinear loads is rapidly increasing in every instance of our business needs. Nearly all these devices are sensitive, minor interruptions in the supply they may not operate properly. Various supplies that degrade Power Quality (PQ) has also been raised. Multiple solutions proposed by different authors overcome the effects caused by PQ issues are accessible. Most attractive one is using power electronic (Inverter) based compensators usually named as Custom Power devices like DSTATCOM, DVR, UPQC, etc. [2] because of the precise role in stimulating medium-voltage high-power appliance, industries developing the electronic devices showing more interest towards the implementation of multilevel inverter (MLI). MLIs are becoming a reputable choice to two-level inverters by their several advantages, such as transformer-less structure, high-power quality signals and less switching losses. Although the harmonics issue is an enormous challenge in this technology, this causes harmful effects on some appliances. Within harmonics, the highly hazardous to the system are lower order harmonics since they create pulsation torque in electric drives, diminish the efficiency, and take down the system lifetime [3-6].

There exists three types conventional topologies related to the multi-level inverters, such as: they are flying capacitors (FCs), neutral point clamped (NPC) and H-bridge cascaded (CHB) [7-9]. The CHB-MLI has many isolated DC excitations, which generates a variable level sinusoidal AC voltage at its output. Several techniques for the modulation of MLI are

detailed in the article that enhances the efficiency of MLI. As per switching frequencies. Sinusoidal pulse-width modulation, conventional modulations have come under high switching. The basic switching frequency technique is more suitable than high-frequency switching techniques for high-power conversion because it having more efficiency in energy conversion. SHEPWM is having superior control over the removal of undesired harmonics in a higher number of levels, and it is efficiently used [10-14].

Numerical, Algebraic, and Evolutionary Algorithms (EAs) are the methods used in SHEPWM [15]. Newton-Raphson (NR), sequential quadratic programming, and gradient optimizations are coming under the numerical techniques, among these Newton-Raphson are the dominating, because it provides precise solutions and converging to optimize solutions at high speed with fewer iterations by providing good initial guesses. However, the selection of the initial guesses is a critical challenge. [16–17]. Groebner bases theory, resultant theory, and Wu methods are coming under algebraic methods. The respective techniques are not preferred for real-time because these are computationally tough, hence used for only low-level inverters [18–19]. The next classification to find optimum firing angles is Evolutionary Algorithms like the Bee (BA), Genetic (GA), and particle swarm optimization (PSO), etc. Implementation of these methods is easy since optimized solutions does not depends on initial guesses and used a fitness function that consists of the fundamental and lower order harmonics relations [20-24]. Switching angles are calculated separately by using GA and PSO in [25] and given as an initial guess to Newton Raphson for the optimized solutions of seven-level inverter. A hybrid PSO-NR and asynchronous PSO-NR algorithms were presented in [26, 27]. The convergence speed is improved by applying a hybrid Mesh Adaptive Direct Search and PSO (MADS-PSO) algorithm in [28]. A reduced switch MLI for standalone RES with SHEPWM was proposed in [29], in this author proposed a PSO algorithm hybrid with fish swarm optimization (FSO). The main objective of the EAs is to reduce the respective fitness function for obtaining the desirable firing angles. The mentioned algorithms have some drawbacks such as the selection criteria for the new population in case of GA, becomes complex in obtaining the local optima with rugged search space in BEE algorithm, low-convergence rate under the iteration process for PSO algorithm. These drawbacks can able to overcome by using the proposed ANN-NR technique.

This paper highlights the-PWM technique accompanying an integrated algorithm it uses the Artificial Neural Network (ANN) and Newton Raphson (NR) method. ANN is trained with optimum switching angles to have been calculated offline, and the estimates generated by the ANN the initial guess for the Newton Raphson method. The input for this inverter is collected from the solar PV and is boosted by using a three-stage boost converter. P&O based MPPT algorithm is used for getting a stable output and a better operation of solar PV.

The work is framed as: the proposed solar PV based Cascaded H bridge MLI with DC-DC converter is enlightened in Section II, SHEPWM switching technique, the procedure of the Newton Raphson method, the architecture of ANN, and the proposed integrated algorithm are discussed in Section III, Simulation and prototype model of proposed topology are executed and the respective results are compared in Section IV, and conclusions are represented in Section V.

II Structure of the Cascaded H-Bridge MLI for PV

The schematic architecture of the H Bridge MLI of a cascaded form for the solar PV application is shown in Fig.1. It comprises cascaded H-Bridge MLI generates the eleven levels output AC voltage by switching IGBTs using a hybrid ANN-NR algorithm based SHE-PMW scheme, and the input is getting from solar PV followed by a three-level DC-DC boost converter. This converter boosts both the respective voltage and MPPT.

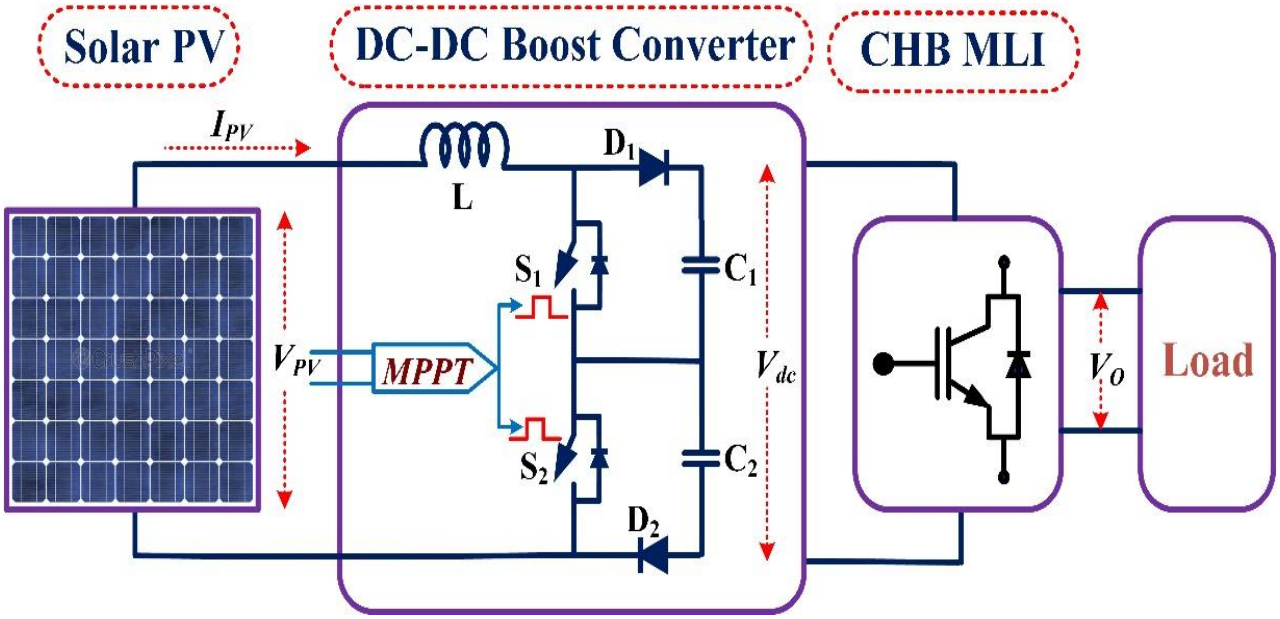

FIGURE 1. Schematic structure of proposed Cascaded H Bridge MLI for solar PV

A. Solar PV Powered Boost Converter

The voltage and currents received from solar PV array directly build upon the irradiance effect, temperature values, number of series and parallel connected strings. Here 1Soltech 1STH-215-P panel with two parallel strings and two series-connected systems per string is selected. The specifications of the selected solar panel are given for one parallel string, and one series-connected system at an irradiance of 1000 W/m2 and 250^{C} temperature is described in TABLE I. Fig. 2 represents the working and control of a three-level boost converter [30,31]. It consists of an inductor L and the dc-link capacitors C_1 and C_2 with two switches S_1 and S_2. The hardware specifications of the respective converter is shown in TABLE I.

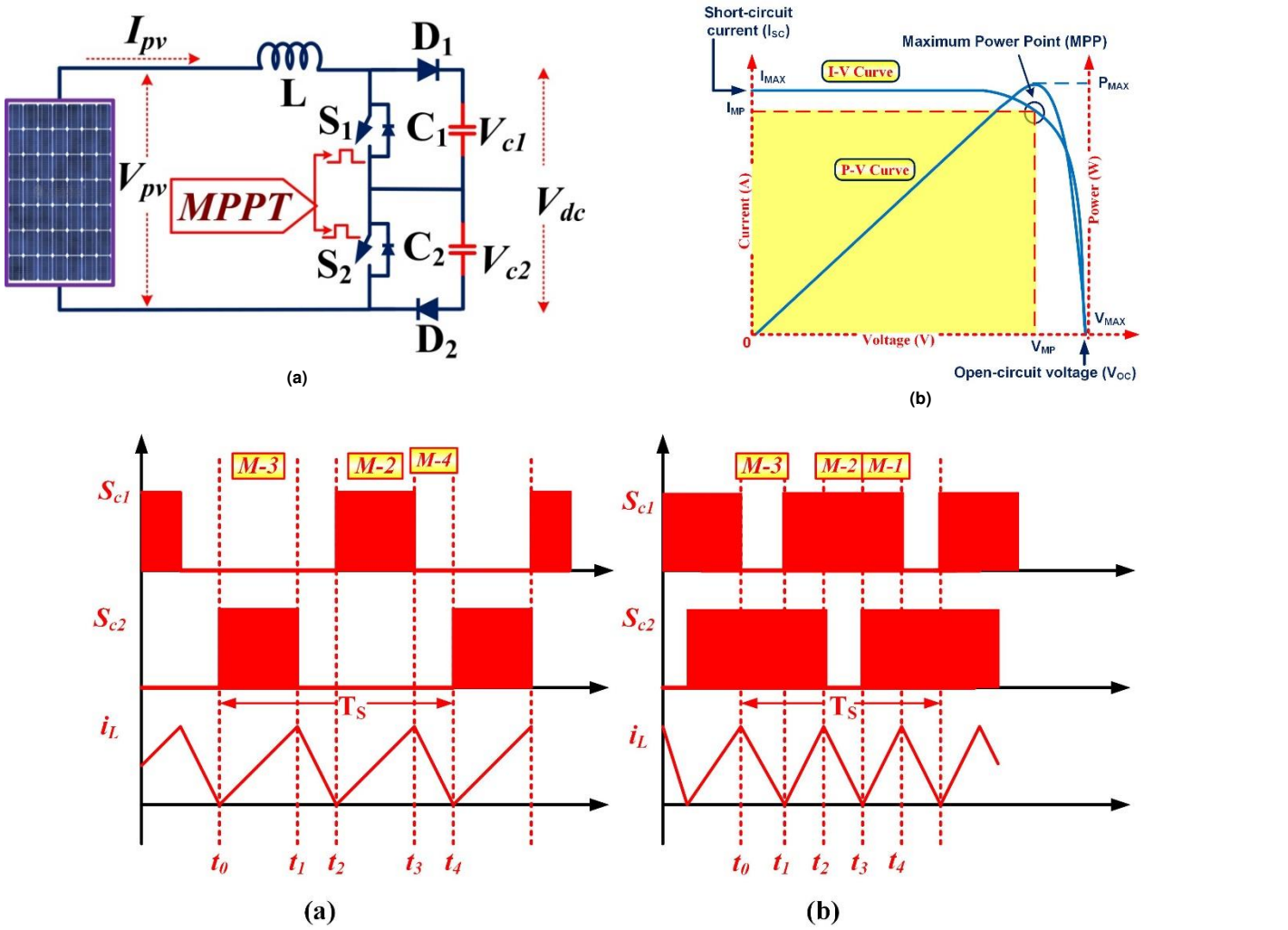

FIGURE 2. (a) Solar-powered three-level boost converter (b) Characteristics of Solar PV (c) Pulses and inductor current for DC-DC boost converter

The proposed three stage boost converter consists of four operating modes such as whenever the switches either S_1 or S_2 turns on, Mode 2 and Mode 3 occurs. Mode 1 and Mode 4 occurs with the switches S_1 and S_2 either turns on or off respectively. There exists two operating modes with respect to the duty ratio D. For duty cycle ($0 < D < 0.869$) the converter allows to work in the respective modes 2, 3, and 4. Whereas for ($0.869 < D < 1$) the boost converter allows to work under Modes 1, 2, and 3. A proper equation showing between PV input source voltage and the dc-link voltage is given by.

$$V_{dc} = \frac{(D \times V_{PV})}{(1-D)} \quad (1)$$

B. MPPT Technology

The maximum power is utilized using P&O technique and determination samples controlled by changing the perturbation count. Fig.3 represents the flowchart of P&O algorithm, which is given as follows

a) From PV, read the values of current I_{pv} and voltage $V_{pv.}$
b) Determine the power $P_{pv} = I_{pv} * V_{pv}$.
c) Store the value of I_{pv} and V_{pv} at the k^{th} instant.
d) Calculated the $(k+1)^{th}$ instant and repeat step 'a'.
e) The values of P_{pv} and V_{pv} at $(k+1)^{th}$ instant are subtracted from the values of k^{th} instant
f) From the power voltage curve, ($dP/dV<0$) is negative for the lower duty cycle (almost to zero) and voltage is nearly constant at the right-side curve and ($dP/dV>0$) is positive for higher duty cycle (nearer to one) in the left side.
g) The polarities of dP and dV decides the increment and decrement of the duty cycle.

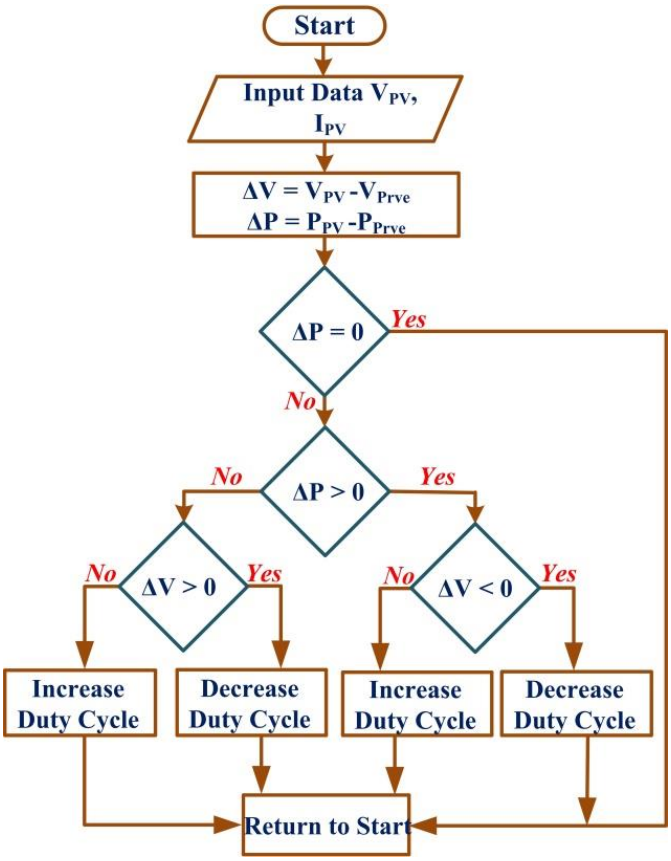

FIGURE 3. Flow-chart of P&O algorithm

TABLE I
SPECIFICATIONS OF 215W PV MODULE & BOOST CONVERTER

PARAMETERS	VALUE
Maximum power	213.15W
Open circuit voltage (V_{oc})	36.3V
Current at maximum power point (I_{mpp})	7.35A
Short circuit current (I_{sc})	7.84A
The voltage at maximum power point (V_{mpp})	29V
Diode saturation current (I_o)	$2.9259*10^{-10}$A
Diode ideality factor	0.98117
Inductance L	15.38 mH
Capacitance C_1 & C_2	282µF
Input DC voltage	~60V
Resistance(R_2)	10 Ohms
Duty Cycle	0.869

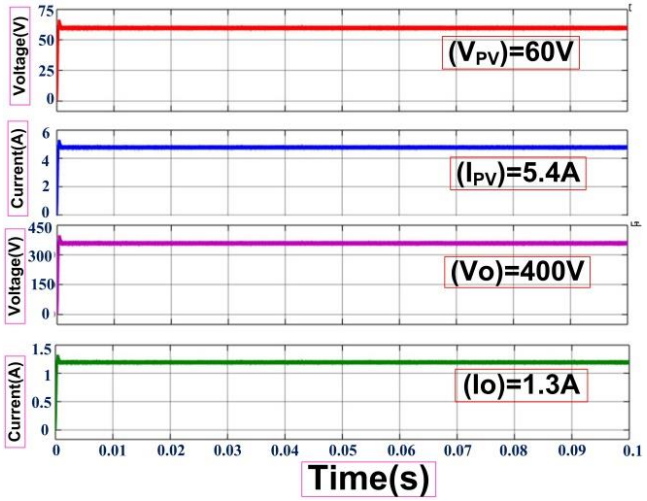

FIGURE 4. Simulation results of PV and boost converter

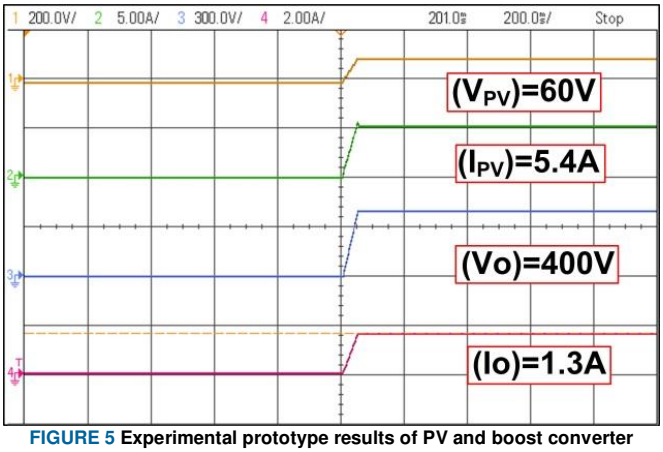

FIGURE 5 Experimental prototype results of PV and boost converter

The designed solar PV provides 60V dc voltage with a 1.3A of current utilizing the solar module 1Soltech 1STH-215-P and the respective voltage gets boosted to 400V utilizing a three-level DC-DC boost converter. Fig. 4 & 5 presents the simulation and experimental results of PV and boost converter, respectively.

C. Cascaded H-Bridge MLI

The multilevel cascade inverter comprises five 1-ϕ full-bridge (H- Bridge) inverters are in series, and it generates a required output voltage. The input of each inverter is taken from dc sources, which is supplied from Solar PV. Fig. 6 (a) shows the generalized structure of a 1-ϕ cascade inverter. By choosing various mixtures of the four number of switches: S_1, S_2, S_3, and S_4 in every inverter, the three number of various voltage levels $+V_{dc}$, zero, and $-V_{dc}$ are getting at AC output side, and the synthesized-out output is the sum of all the individual 1-ϕ H—Bridge inverter outputs. Let S is the number of dc sources then 2S+1 is voltage levels got in a CHBML inverter. The eleven level CHBML inverter five H Bridges is shown in Fig. 6 (a) & (b). The output voltage is given by.

$$V_{an} = V_1 + V_2 + V_3 + V_4 + V_5 \quad (2)$$

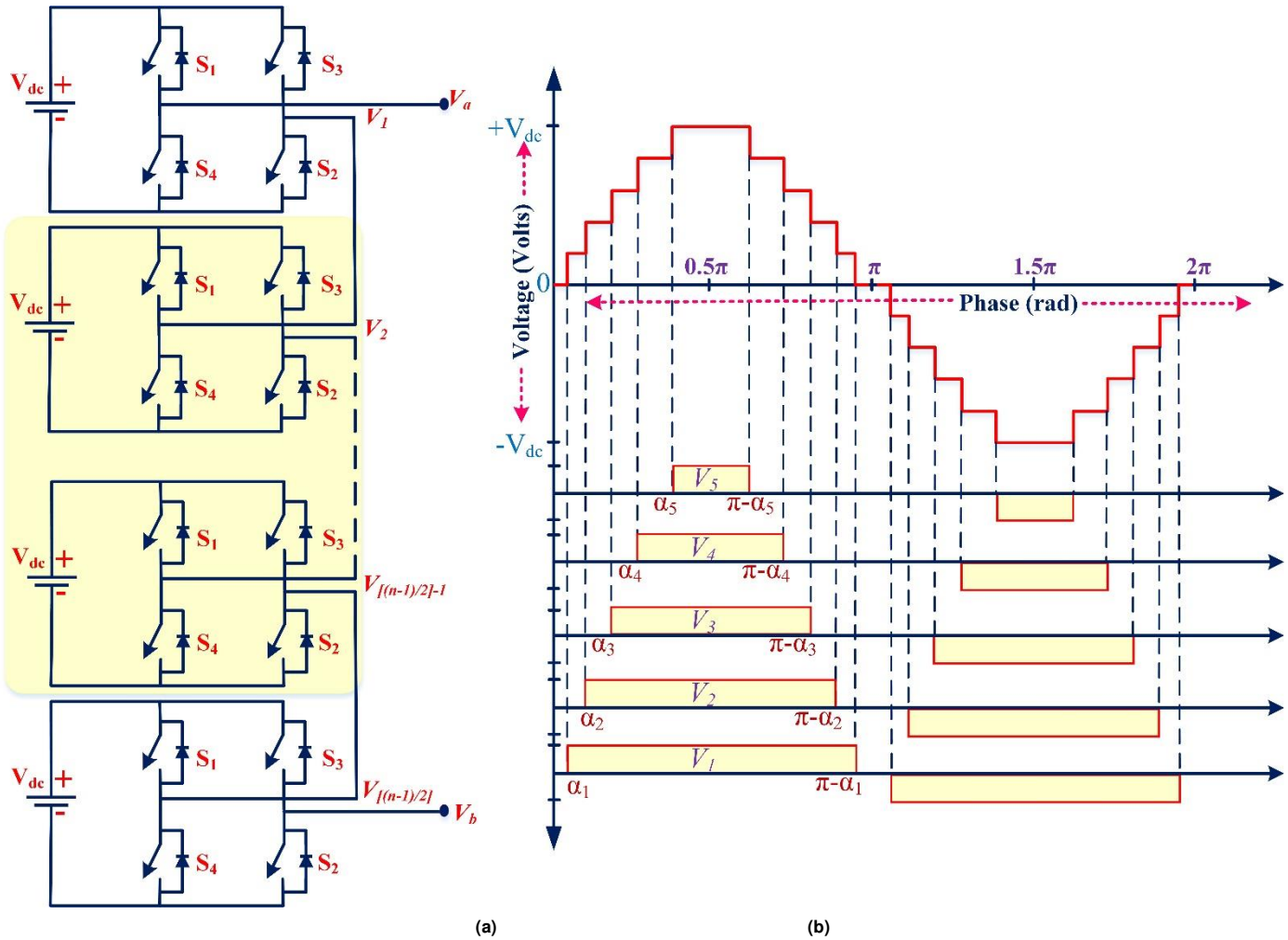

(a) (b)

FIGURE 6. (a) Cascaded H Bridge MLI, (b) 11 level output voltage waveform of Cascaded H Bridge MLI

III SHEPWM Technique

In this SHEPWM technique, the output voltage of the CHBMLI inverter is expressed using the equation 3.

$$f_n(t) = A_0 + \sum_{n=1}^{S}(A_n \cos(n\omega t) + V_n \sin(n\omega t)) \quad (3)$$

Where Ao is the DC component, i.e.

$$A_o = \frac{1}{2\pi}\int_0^{2\pi} f(t) \quad (4)$$

A_n represents even harmonics,

$$A_n = \frac{1}{\pi}\int_0^{2\pi} f(t)\sin n\omega t \; dt \quad (5)$$

V_n denotes odd harmonics,

$$V_n = \frac{1}{\pi}\int_0^{2\pi} f(t)\cos n\omega t \; dt \quad (6)$$

The obtaining of an efficient output can be done with less frequency switching. Hence, the undesired lower order harmonics are removed from the output and is constrained to (S−1). In order to remove the respective undesired harmonic content, the increase of levels count should happen in a precise way. As the inverter output is quarter symmetrical, DC devices, even harmonics becomes null. Hence the equation 3 is simplified as:

$$f_n(t) = V_n \sin(n\alpha_i) \quad (7)$$

Where V_n is expressed from the equation (8):

$$V_n = \frac{4V_{dc}}{n\pi}\sum_{i=1}^{s}((-Q_i)^{i+1}\cos(n\alpha_i)) \quad (8)$$

Where V_{dc} is the optimal DC voltage and $Q_i = \frac{V_{dci}}{V_{dc}}$, V_{dci} is the DC voltage source.

$$V_n = \frac{4V_{dc}}{n\pi}[Q_1\cos(n\alpha_1) \pm Q_2\cos(n\alpha_2) \pm Q_3\cos(n\alpha_3) \pm --- \pm Q_s\cos(n\alpha_s)] \quad (9)$$

From the above relation,'+' sign indicates the increasing edge, and '-' sign indicates decreasing edge. Several switching angles are combined in order to form a stepped waveform, which can be further classified into the levels of modulation index. The minimization of harmonics results in the formation of less frequency switching can be obtained by using various modulation indices. The basic equations for the, 5th, 7th, 11th, and 13th order harmonic, and for the modulation index (M) of the developed 11-level inverter are given in equation (10):

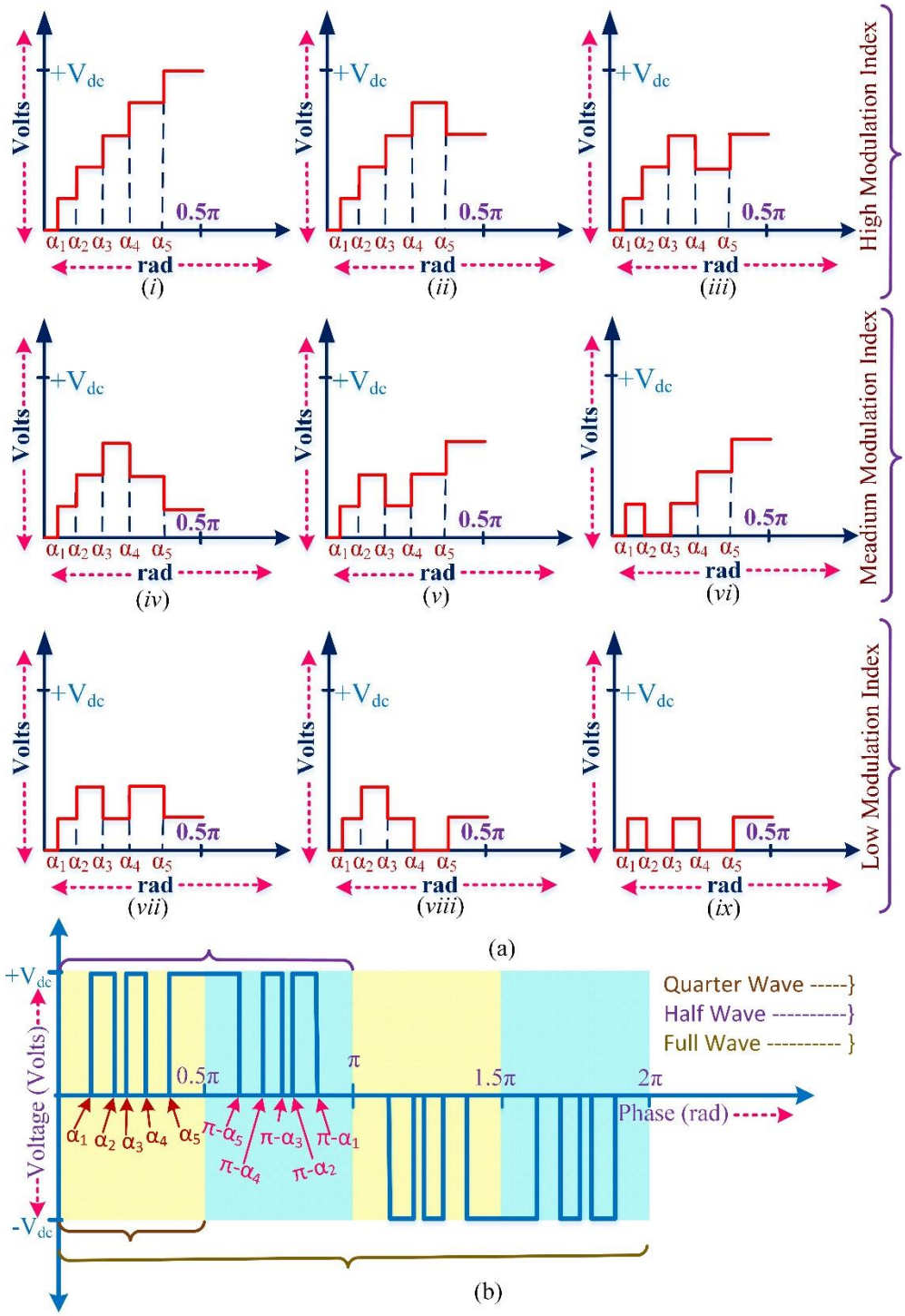

FIGURE 7. 11 level output voltage waveforms with different modulation indexes. (a) Synthesis of Various Patterns (b) Extending waveform

$$\left.\begin{aligned} V_{fun} &= \frac{4V_{dc}}{\pi}\left[\cos(\alpha_1)+\cos(\alpha_2)+\cos(\alpha_3)+\cos(\alpha_4)+\cos(\alpha_5)\right] \\ V_{5th} &= \frac{4V_{dc}}{5\pi}\left[\cos(5\alpha_1)+\cos(5\alpha_2)+\cos(5\alpha_3)+\cos(5\alpha_4)+\cos(5\alpha_5)\right] \\ V_{7th} &= \frac{4V_{dc}}{7\pi}\left[\cos(7\alpha_1)+\cos(7\alpha_2)+\cos(7\alpha_3)+\cos(7\alpha_4)+\cos(7\alpha_5)\right] \\ V_{11th} &= \frac{4V_{dc}}{11\pi}\left[\cos(11\alpha_1)+\cos(11\alpha_2)+\cos(11\alpha_3)+\cos(11\alpha_4)+\cos(11\alpha_5)\right] \\ V_{13th} &= \frac{4V_{dc}}{13\pi}\left[\cos(13\alpha_1)+\cos(13\alpha_2)+\cos(13\alpha_3)+\cos(13\alpha_4)+\cos(13\alpha_5)\right] \\ M &= \frac{\pi V_D}{4SV_{dc}} \end{aligned}\right\} \quad (10)$$

Where V_D is the fundamental voltage. In the SHEPWM technique, the reliable switching angles (α_1, α_2, α_3, α_4, and α_5) of the proposed inverter are obtained using the equation (11):

$$\left.\begin{aligned} M = \frac{1}{5}\left[\cos(\alpha_1) + \cos(\alpha_2) + \cos(\alpha_3) + \cos(\alpha_4) + \cos(\alpha_5)\right] \\ \left[\cos(5\alpha_1) + \cos(5\alpha_2) + \cos(5\alpha_3) + \cos(5\alpha_4) + \cos(5\alpha_5)\right] = 0 \\ \left[\cos(7\alpha_1) + \cos(7\alpha_2) + \cos(7\alpha_3) + \cos(7\alpha_4) + \cos(7\alpha_5)\right] = 0 \\ \left[\cos(11\alpha_1) + \cos(11\alpha_2) + \cos(11\alpha_3) + \cos(11\alpha_4) + \cos(11\alpha_5)\right] = 0 \\ \left[\cos(13\alpha_1) + \cos(13\alpha_2) + \cos(13\alpha_3) + \cos(13\alpha_4) + \cos(13\alpha_5)\right] = 0 \end{aligned}\right\} \quad (11)$$

The respective firing angles can be calculated by using equation (10) must satisfy the relations provided in the equation (12):

$$0 \le \alpha_1 \le \alpha_2 \le \alpha_3 \le \alpha_4 \le \alpha_5 \le \frac{\pi}{2} \quad (12)$$

The proposed MLI is operated at the fundamental frequency with five sources; hence the possibility of different switching patterns is 2^5=32. Among these only 9 patterns the corrected waveforms shown in Fig. 7(a), and 16 patterns are a mirror image to the horizontal axis. Because of symmetry, the only one-quarter waveform is shown in Fig.7 (a), and the respective waveform considering quarter and half-wave symmetries shown in Fig.7 (b). The result of the SHEPWM equations is complicated because of its nonlinear transcendental nature. Therefore, the selected harmonic content can be removed with the obtained solutions.

A. Newton Raphson (NR) Method

The proposed Newton Raphson method is implemented by assuming a random initial guess which is in between 0 to 90^0, the iterations count is j and ε.

An algorithm for optimizing switching angles is.

1. Guess a set of initial estimates for switching angles $\alpha^0 = [\alpha_1^0, \alpha_2^0, \alpha_3^0, \ldots, \alpha_n^0]$
2. Compute the values for the constraint equations, the Jacobian matrix for the set of equations and dα

$$J = \begin{bmatrix} \frac{\partial f_1}{\partial \alpha_1} & \cdots & \frac{\partial f_1}{\partial \alpha_n} \\ \vdots & \ddots & \vdots \\ \frac{\partial f_m}{\partial \alpha_1} & \cdots & \frac{\partial f_m}{\partial \alpha_m} \end{bmatrix} \quad (13)$$

$$d\alpha = J * f(\alpha^k) \quad (14)$$

for 'n' variables in the 'k' iterations, using' distinct equations.

3. While the tolerance ε is less than dα, repeat step 4. If the tolerance is greater than or equal to dα, end the process.
4. Update α using Eq. 15 and return to Step 2.

$$\alpha^{k+1} = \alpha^k + d\alpha \quad (15)$$

B. Artificial Neural Network

The proposed ANN comprises one input layer which is fed with voltage V_{dc} of each stage, two hidden layers interconnected with the input and the output layer, and the output layer generates optimal or near-optimal values for switching angles for each step of the multilevel inverter. Here, 'tanh' activation function is used for introducing nonlinearity to the model, and the range of 'tanh' function is from -1 to 1. The proposed architecture of ANN is shown in Fig. 8.

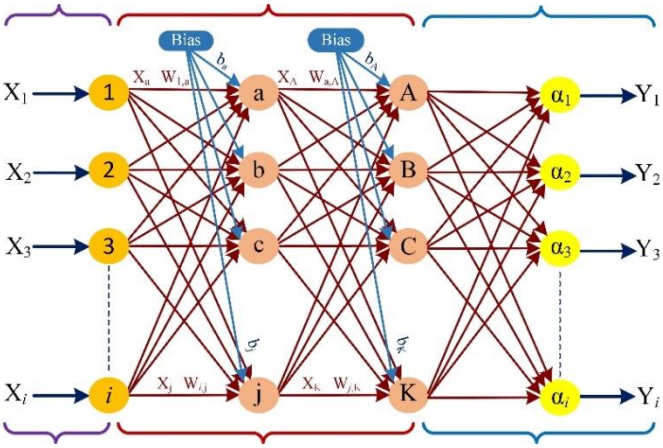

FIGURE 8. ANN architecture

Each neuron Y_i calculates a weighted sum of all its inputs X_k, where k ranges from zero to the number of neurons present in the previous layer. An activation function applies to scale all output values between a ranges. Mathematically, it is expressed as

$$Y_i = \tanh(W_k X_k + B_i) \quad (16)$$

Where W_K is the weight associated with each neuron of the previous layer, X_K is the output of the k^{th} neuron in the last layer, and B_i is the bias added in the layer i. Performance and error metrics can be calculated using mean squared error loss expressed in Eq.17. Adam optimizer is used to reduce loss by modifying the weights of each layer through a process called Back Propagation.

$$\text{Mean squared error} = \frac{1}{N}\sum_{i=1}^{N}(y_i - \hat{y}_i)^2 \quad (17)$$

C. Proposed ANN-NR Method

In the proposed approach, the artificial neural network is trained with optimum switching angle data that has been calculated offline for a specific inverter configuration, here the neural network is trained by splitting the data into training, testing, and validation sets in the ratio of 60:20:20. The estimates generated by the neural network the initial guess for further optimization using the Newton Raphson method. Since the estimated generated by the artificial neural network are close to the global optima, it results in rapid convergence and extremely accurate figures for switching angles. In case perfect solutions do not exist for the set of equations, the solutions from the neural networks work as sufficiently precise switching angles, resulting in defective harmonic components. The

This article has been accepted for publication in a future issue of this journal, but has not been fully edited. Content may change prior to final publication. Citation information: DOI 10.1109/ACCESS.2021.3081460, IEEE Access

process of optimization for the proposed hybrid ANN-NR algorithm is described by the flowchart shown in Fig 9.

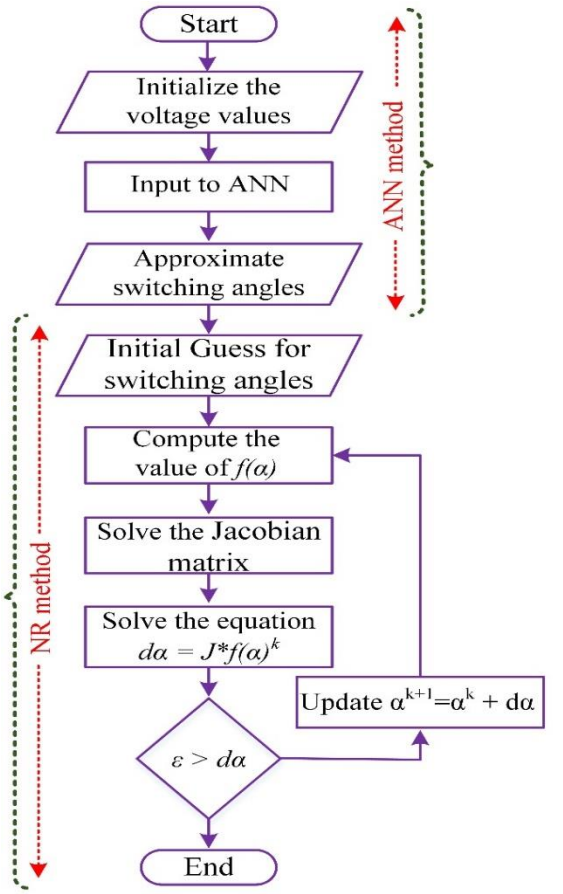

FIGURE 9. Flow chart for the Proposed ANN-NR algorithm

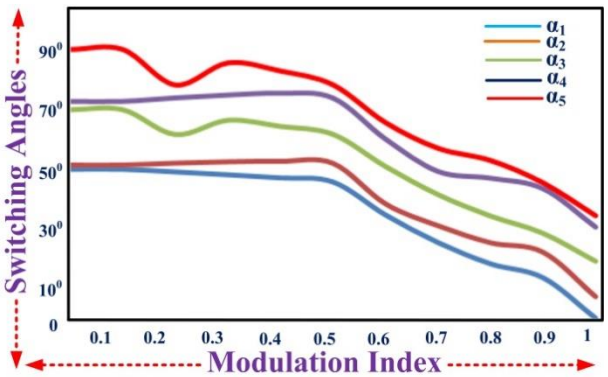

FIGURE 10. Switching angles for eleven levels

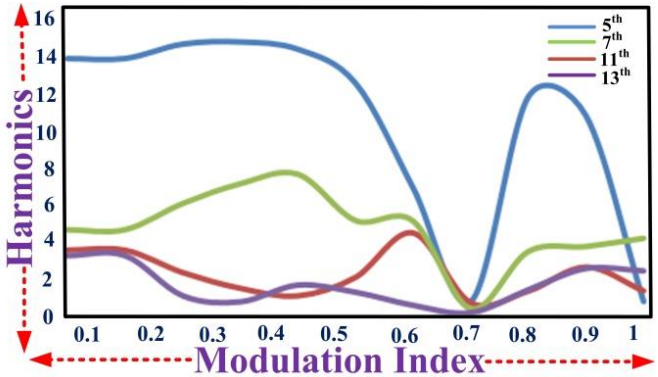

FIGURE 11. Harmonics order for eleven levels

TABLE II
SWITCHING ANGLES AND HARMONIC ANALYSIS FOR 11-LEVEL WITH DIFFERENT MI

MI	α_1	α_2	α_3	α_4	α_5	5^{th}	7^{th}	11^{th}	13^{th}
0.1	49.21153	50.62675	68.52602	71.16163	88.12125	14.03	3.52	4.67	3.23
0.2	48.35209	51.26846	60.44728	72.30755	76.60475	14.82	2.31	6.1	1.05
0.3	47.4239	51.70391	65.08826	73.22429	83.76675	14.94	1.46	7.18	0.72
0.4	46.40976	51.87007	63.0829	73.79725	81.13114	14.54	1.05	7.7	1.63
0.5	45.08049	51.20544	60.50458	72.25026	76.66205	12.68	2.05	5.17	1.24
0.6	34.31457	37.92995	50.03087	58.95758	64.4007	6.93	4.45	5.14	0.53
0.7	25.29045	30.75649	40.86351	48.4495	56.05841	0.69	0.68	0.35	0.13
0.8	18.35191	25.17586	33.8734	46.2436	52.09925	11.93	1.31	3.48	1.38
0.9	13.80261	22.08761	28.24693	42.85168	44.83412	10.89	2.61	3.75	2.53
1	0.57869	7.500046	19.13113	30.40126	34.17706	0.69	1.32	4.2	2.4

TABLE III
THD AND HARMONIC COMPARISON BETWEEN PROPOSED TOPOLOGY AND OTHER TOPOLOGIES

Topologies	Levels	MI	3^{rd}	5^{th}	7^{th}	11^{th}	13^{th}	THD
NLC	7	0.63	4.89	1.18	-	-	-	18.12
SHEPWM (APSO-GA) [32]	7	0.81	0.01	0.00	-	-	-	11.48
SHEPWM (PSO) [33]	9	0.65	-	-	-	-	-	11.0
SHEPWM (PSO) [34]	9	0.65	-	-	-	-	-	11.75
SHEPWM (ANN-NR) [Proposed]	9	0.69	-	0.91	0.80	0.53	0.32	11.56
	11	0.69	-	0.69	0.68	0.35	0.13	9.1

This article has been accepted for publication in a future issue of this journal, but has not been fully edited. Content may change prior to final publication. Citation information: DOI 10.1109/ACCESS.2021.3081460, IEEE Access

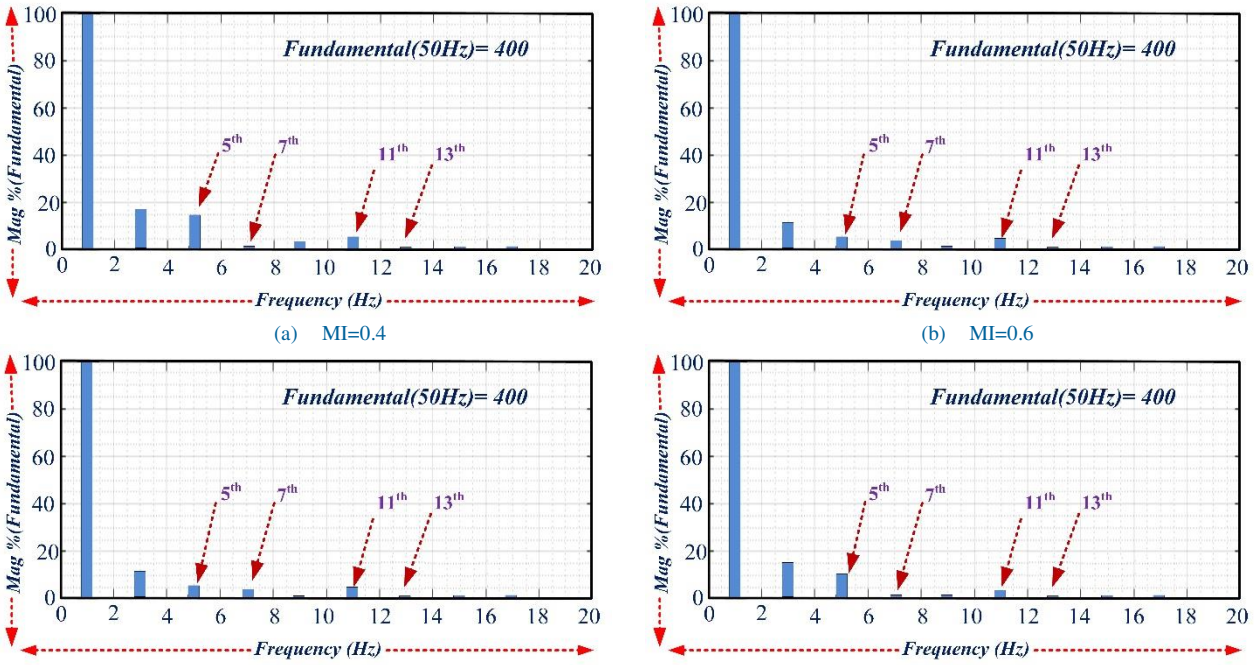

(a) MI=0.4 (b) MI=0.6

(c) MI=0.69 (d) MI=0.8

FIGURE 12. FFT analyses at different MI for eleven levels inverter

The variation of the parameters like modulation index and THD with harmonic spectrum is compared with various topologies and is represented in Table III. It is found that the THD of the proposed topology holds the best in its outcome with a lesser value. The harmonic spectrum at different modulation index are shown in Fig 12.

IV Results and Discussions

A. Simulation Results

The proposed hybrid ANN-NR algorithm is formulated in MATLAB for obtaining five (α_1, α_2, α_3, α_4, α_5) optimized switching angles and the respective results of the developed inverter are represented in Fig 10. Here, the switching angles are generated and having equal input voltage sources and the modulation index is in between ($0 \leq MI \leq 1$). By utilizing the FFT tool in MATLAB/ Simulink, the results of the harmonic analysis are presented in Fig 11, it represents that in the 11-level inverter the 5th, 7th, 11th, and 13th harmonics are removed from the output under the specific range of MI. TABLE II represents the switching angles and harmonic analysis for different MI. In the range from 0.68 to 0.72 MI, the switching angles of eleven level inverter are optimum, and they are α_1= 25.290^0, α_2= 30.756^0, α_3= 40.863^0, α_4= 48.45^0, and α_5= 56.06^0 at these angles the 5th, 7th, 11th, and 13th harmonics are removed, and the FFT analysis at MI=0.69 for eleven levels is presented in Fig 12. The simulation output voltage of 7-, 9-, and 11-levels is shown in Fig 13 (a), (b) & (c) respectively, and the simulation output of voltage and current of 11 levels is presented in Fig 14.

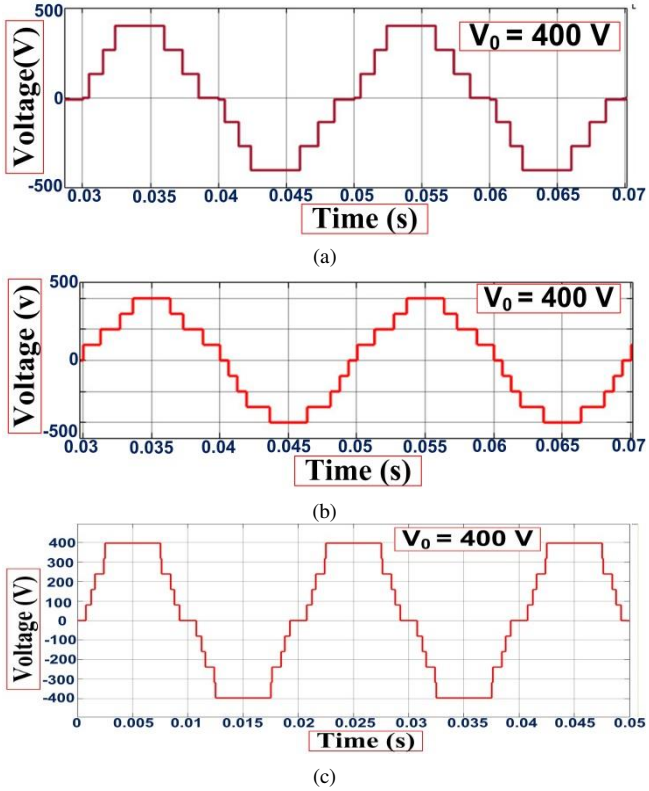

(a)

(b)

(c)

FIGURE 13. The simulation output voltage of (a) seven (b) nine (c) eleven level Inverter

This article has been accepted for publication in a future issue of this journal, but has not been fully edited. Content may change prior to final publication. Citation information: DOI 10.1109/ACCESS.2021.3081460, IEEE Access

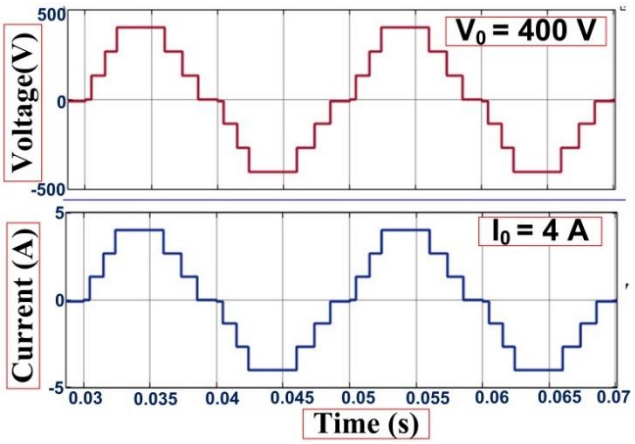

(a)

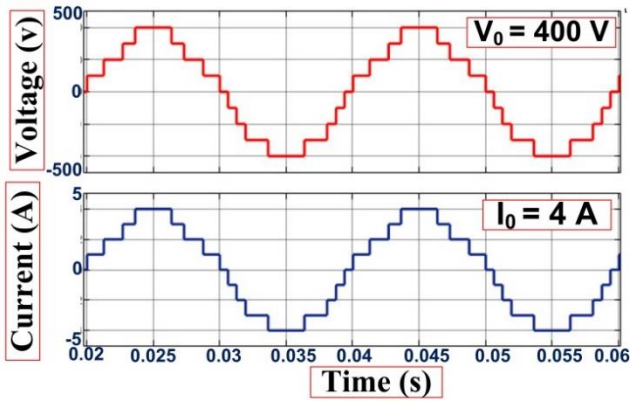

(b)

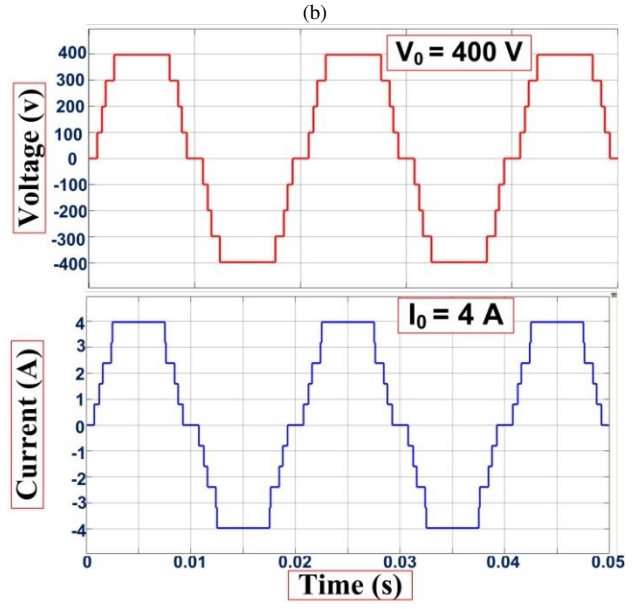

(c)

FIGURE 14. Simulation output voltage and current of eleven level Inverter

B. Experimental Results

For implement this in real-time applications, a PV based system is shown in Fig 15. The switches were controlled by the pulse pattern generated by using the ANN-NR control algorithm in Simulink/MATLAB and downloaded on a dSPACE RTI1104 system. Depends on the desired output, DS1104 produces the pulses with respect to the switching angles for MI are tabulated and provided to the gate drives using digital I/O ports in order to operate the IGBTs and also it provides isolation through the MCT2E optocoupler. The simulation results are experimentally verified by developing the eleven-level inverter setup. IKW75N60T, 600V, 75A IGBT is used for CHBMLI with 50Hz frequency, in order to operate the IGBTs the pulses need to be generated using a dSPACE RTI1104 controller.

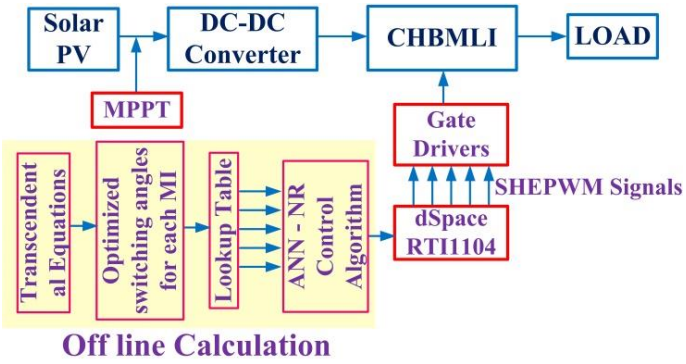

FIGURE 15. ANN-NR based SHEPWM for solar PV.

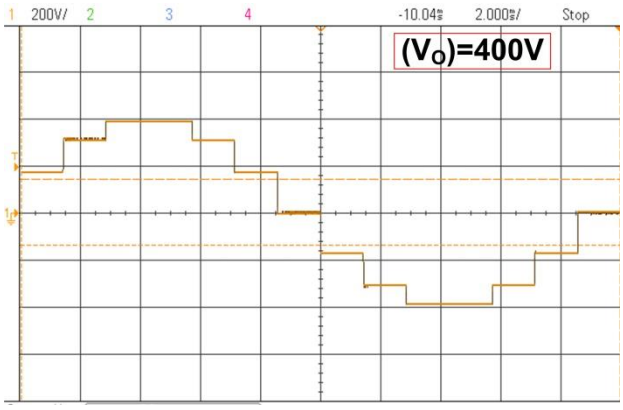

(a)

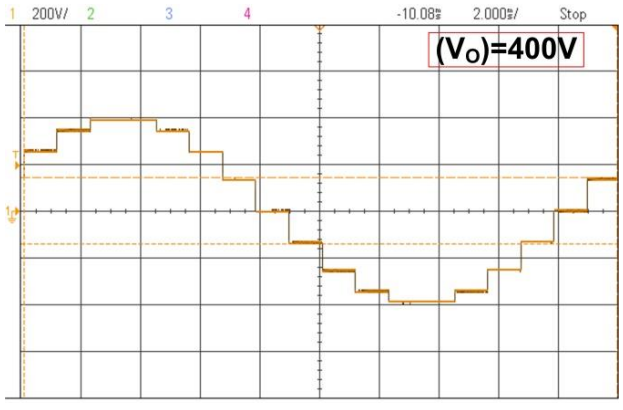

(b)

This article has been accepted for publication in a future issue of this journal, but has not been fully edited. Content may change prior to final publication. Citation information: DOI 10.1109/ACCESS.2021.3081460, IEEE Access

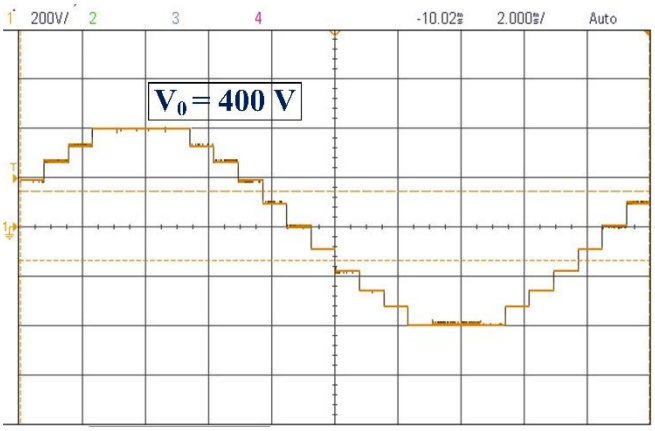

(c)

FIGURE 16. The experimental output voltage of (a) seven (b) nine (c) eleven level Inverter

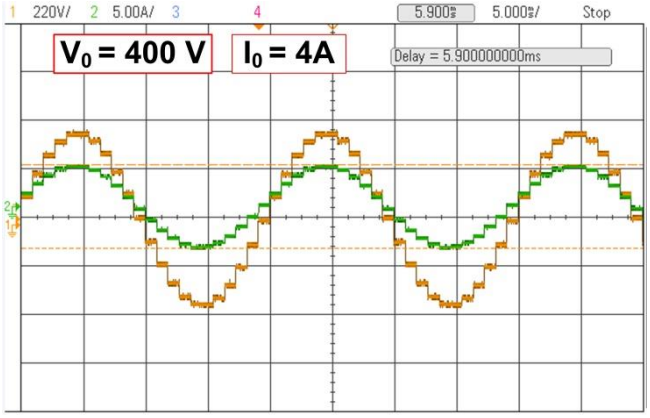

FIGURE 17. Experimental output voltage and current of eleven level Inverter

The hardware output voltage of 7, 9, and 11 levels and output voltage and currents of the 11-levels are shown in Fig 16 (a), (b) & (c) and Fig 17. Fig 18 presents the experimental THD of 11 level converter.

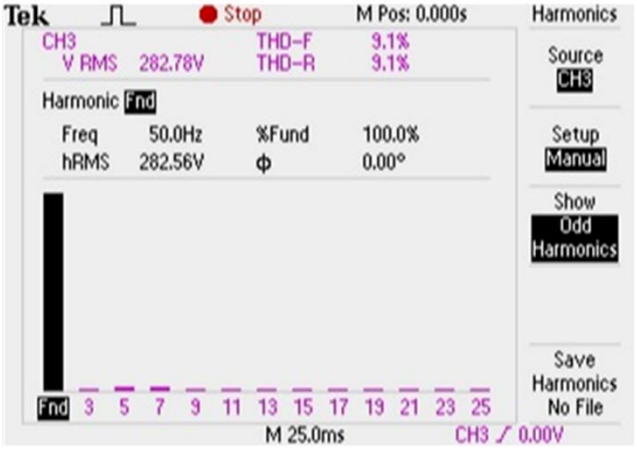

FIGURE 18. Experimental THD of eleven level Inverter

TABLE IV
COMPONENT SPECIFICATIONS

Parameter	Symmetric	Asymmetric
No. of voltage Source	5	3
No. of switches	20	12
Load Resistance	80Ω	80Ω
Output Voltage (Vo)	Vrms = 282.84V	Vrms = 282.84 V
Output Current (Io)	Irms=3.53A	Irms=3.53 A
IGBTs (CM75DU-12H)	600 V, 75 A	600 V, 75 A
dSPACE Controller	RTI1104	RTI1104
Driver circuit	TLP250	TLP250
Programmable DC sources	500 V	500 V

V Power Loss and Efficiency

The losses are majorly classified into two types like switching and conduction losses with respect to the switches. Therefore, the conduction losses comes to the role under the switching conditions when turns on at all instants and these are calculated using the equation (18).

$$P_{Cls} = [V_S + R_S i^{\alpha}(t)]\, i(t) \quad (18)$$

Where V_S and V_d are the respective voltages at the various switches and diodes respectively. The resistance for the switch is represented as R_S and the diode resistance is R_d. Therefore, the generalized relation for obtaining conduction losses (P_{cl}) by the consideration of the number of switches and diodes N_{IGBT} and N_d respectively at time t is given according to the equation (19).

$$P_{Cl} = \frac{1}{2\pi}\int_0^{2\pi}\left[N_{IGBT}(t)P_{cl,IGBT}(t)\, dt\right] \quad (19)$$

The calculation of switching losses can be done using the following relation (20)

$$P_{Sl} = f\sum_{K=1}^{N_{switch}}\left[\sum_{j=1}^{N_{on,k}} En_{on,kj} + \sum_{j=1}^{N_{off,k}} En_{off,kj}\right] \quad (20)$$

Where E_{on} and E_{off} are the utilized energies by the switches under conduction state.

The overall power losses $(P_{total\ loss})$ are calculated according to the following relation

$$P_{total\ loss} = P_{cl} + P_{sl} \quad (21)$$

The overall efficiency (η) of the topology can be determined using the equation (22)

$$\eta = \frac{P_{out}}{P_{in}} = \frac{P_{out}}{P_{out}+P_{loss}} \quad (22)$$

where P_{out} and P_{in} are the output and input powers.

The respective power output is determined using equation (23)

$$P_{out} = V_{rms} * I_{rms} \quad (23)$$

TABLE V
POWER LOSS AND EFFICIENCY CALCULATIONS

	Symmetric	Asymmetric
Conduction loss (w)	97.45	58.47
Switching loss (w)	0.284	0.170
Total losses (w)	97.73	58.64
Output power (w)	795.8	795.8
Input power (w)	890.5	854.4
Efficiency (%)	89.39	93.14

The hardware specifications of the developed topology are represented in Table IV. The power loss and efficiency of the developed topology with respect to the symmetric and

asymmetric configurations are determined and tabulated in Table V. In the asymmetrical configuration, the three DC sources are considered with a ratio of 1:2:2.

VI Conclusion

This paper, a hybrid Artificial Neural Network - Newton Raphson (ANN-NR) was implemented to mitigate the lower order harmonics in the H-Bridge cascaded MLI for solar photovoltaic (PV). Optimum selection of switching angles was made by employing the SHE-PWM technique accompanying an integrated algorithm; hence the respective harmonics are optimized and curtail the THD value. ANN is trained with optimum switching angles, and the estimates generated by the ANN were the initial guess for NR. In this paper, the CHB-MLI was combined with a traditional boost converter; it boosts the PV voltage to a higher dc-link voltage. P&O based MPPT algorithm is utilized for obtaining a stable output and efficient operation of solar PV. The developed technique is tested for the proposed inverter, the simulation is performed in Matlab/Simulink and the respective results confirmed that the developed algorithm is efficient, and offered highly precise firing angles with a few iterations having the increased capability of tackling local optima values. The developed algorithm is verified by using an experimental implementation of the proposed H-bridge inverter. The proposed SHE-PWM algorithm well suits for grid-connected applications and FACTS.

REFERENCES

[1] Ozdemir, Engin, Sule Ozdemir, and Leon M. Tolbert. “Fundamental-frequency-modulated six-level diode-clamped multilevel inverter for three-phase standalone photovoltaic system.” IEEE Transactions on Industrial Electronics 56, no. 11 (2008): 4407-4415.

[2] Bana, Prabhat Ranjan, Kaibalya Prasad Panda, and Gayadhar Panda. “Power quality performance evaluation of multilevel inverter with reduced switching devices and minimum standing voltage.” IEEE Transactions on Industrial Informatics 16.8 (2019): 5009-5022.

[3] Lashab, Abderezak, Dezso Sera, Frederik Hahn, Luis Camura, Marco Liserre, and Josep Guerrero. “A Reduced Power Switches Count Multilevel Converter-Based Photovoltaic System with Integrated Energy Storage.” IEEE Transactions on Industrial Electronics (2020).

[4] Wang, Lei, Q. H. Wu, and Wenhu Tang. “Novel cascaded switched-diode multilevel inverter for renewable energy integration.” IEEE transactions on energy conversion 32, no. 4 (2017): 1574-1582.

[5] Ahmed, Ashraf, Mohana Sundar Manoharan, and Joung-Hu Park. “An efficient single-sourced asymmetrical cascaded multilevel inverter with reduced leakage current suitable for single-stage PV systems.” IEEE Transactions on Energy Conversion 34, no. 1 (2018): 211-220.

[6] Faraji, Faramarz, Aliakbar Motie Birjandi, Xiao Qiang Guo, B. Wang, and Jianhua Zhang. “An Improved Multilevel Inverter for Single-Phase Transformerless PV System.” IEEE Transactions on Energy Conversion (2020).

[7] Bana, Prabhat Ranjan, Kaibalya Prasad Panda, R. T. Naayagi, Pierluigi Siano, and Gayadhar Panda. “Recently developed reduced switch multilevel inverter for renewable energy integration and drives application: topologies, comprehensive analysis and comparative evaluation.” IEEE access 7 (2019): 54888-54909.

[8] Dhanamjayulu, C., and S. Meikandasivam. “Implementation and comparison of symmetric and asymmetric multilevel inverters for dynamic loads.” IEEE Access 6 (2017): 738-746.

[9] Hamzeh, Mohsen, Amin Ghazanfari, Hossein Mokhtari, and Houshang Karimi. “Integrating hybrid power source into an islanded MV microgrid using CHB multilevel inverter under unbalanced and nonlinear load conditions.” IEEE Transactions on energy Conversion 28, no. 3 (2013): 643-651.

[10] Dahidah, Mohamed SA, Georgios Konstantinou, and Vassilios G. Agelidis. "A review of multilevel selective harmonic elimination PWM: formulations, solving algorithms, implementation and applications." *IEEE Transactions on Power Electronics* 30, no. 8 (2014): 4091-4106.

[11] Li, Li, Dariusz Czarkowski, Yaguang Liu, and Pragasen Pillay. "Multilevel selective harmonic elimination PWM technique in series-connected voltage inverters." *IEEE Transactions on Industry Applications* 36, no. 1 (2000): 160-170.

[12] Davison, Andrew J., Ian D. Reid, Nicholas D. Molton, and Olivier Stasse. "MonoSLAM: Real-time single camera SLAM." *IEEE transactions on pattern analysis and machine intelligence* 29, no. 6 (2007): 1052-1067.

[13] Moeini, Amirhossein, Hossein Iman-Eini, and Mohamadkazem Bakhshizadeh. "Selective harmonic mitigation-pulse-width modulation technique with variable DC-link voltages in single and three-phase cascaded H-bridge inverters." *IET Power Electronics* 7, no. 4 (2013): 924-932.

[14] Dahidah, Mohamed SA, Georgios Konstantinou, and Vassilios G. Agelidis. "A review of multilevel selective harmonic elimination PWM: formulations, solving algorithms, implementation and applications." *IEEE Transactions on Power Electronics* 30, no. 8 (2014): 4091-4106.

[15] Memon, Mudasir Ahmed, Saad Mekhilef, Marizan Mubin, and Muhammad Aamir. “Selective harmonic elimination in inverters using bio-inspired intelligent algorithms for renewable energy conversion applications: A review.” Renewable and Sustainable Energy Reviews 82 (2018): 2235-2253.

[16] Enjeti, Prasad N., Phoivos D. Ziogas, and James F. Lindsay. “Programmed PWM techniques to eliminate harmonics-A critical evaluation.” Conference Record of the 1988 IEEE Industry Applications Society Annual Meeting. IEEE, 1988.

[17] Sun, Jian, Stephan Beineke, and Horst Grotstollen. “Optimal PWM based on real-time solution of harmonic elimination equations.” IEEE Transactions on Power Electronics 11.4 (1996): 612-621.

[18] Yang, Kehu, Qi Zhang, Ruyi Yuan, Wensheng Yu, Jiaxin Yuan, and Jin Wang. “Selective harmonic elimination with Groebner bases and symmetric polynomials.” IEEE transactions on Power Electronics 31, no. 4 (2015): 2742-2752.

[19] Chiasson, John N., Leon M. Tolbert, Keith J. McKenzie, and Zhong Du. “Control of a multilevel converter using resultant theory.” IEEE Transactions on control systems technology 11, no. 3 (2003): 345-354.

[20] Amjad, Abdul Moeed, and Zainal Salam. “A review of soft computing methods for harmonics elimination PWM for inverters in renewable energy conversion systems.” Renewable and Sustainable Energy Reviews 33 (2014): 141-153.

[21] Trzynadlowski, Andrej M., and Stanislaw Legowski. "Application of neural networks to the optimal control of three-phase voltage-controlled inverters." *IEEE transactions on power electronics* 9, no. 4 (1994): 397-404.

[22] Trzynadlowski, A. M., and C. Gang. "Computation of optimal switching patterns for voltage-controlled inverters using neural-network software." In *[Proceedings] 1992 IEEE Workshop on Computers in Power Electronics*, pp. 229-237. IEEE, 1992.

[23] Maia, Helder Zandonadi, Tiago HA Mateus, Burak Ozpineci, Leon M. Tolbert, and João OP Pinto. "Adaptive selective harmonic minimization based on ANNs for cascade multilevel inverters with varying DC sources." *IEEE transactions on Industrial Electronics* 60, no. 5 (2012): 1955-1962.

[24] Tolbert, Leon M., Yue Cao, and Burak Ozpineci. "Real-time selective harmonic minimization for multilevel inverters connected to solar panels using artificial neural network angle generation." *IEEE Transactions on industry applications* 47, no. 5 (2011): 2117-2124.

[25] Barkati, Said, Lotfi Baghli, El Madjid Berkouk, and Mohamed-Seghir Boucherit. “Harmonic elimination in diode-clamped multilevel

inverter using evolutionary algorithms." Electric Power Systems Research 78, no. 10 (2008): 1736-1746.
[26] Shen, Ke, Dan Zhao, Jun Mei, Leon M. Tolbert, Jianze Wang, Mingfei Ban, Yanchao Ji, and Xingguo Cai. "Elimination of harmonics in a modular multilevel converter using particle swarm optimization-based staircase modulation strategy." IEEE Transactions on Industrial Electronics 61, no. 10 (2014): 5311-5322.
[27] Memon, Mudasir Ahmed, Saad Mekhilef, and Marizan Mubin. "Selective harmonic elimination in multilevel inverter using hybrid APSO algorithm." IET Power Electronics 11.10 (2018): 1673-1680.
[28] Routray, Abhinandan, Rajeev Kumar Singh, and Ranjit Mahanty. "Harmonic minimization in three-phase hybrid cascaded multilevel inverter using modified particle swarm optimization." IEEE Transactions on Industrial Informatics 15.8 (2018): 4407-4417.
[29] Panda, Kaibalya Prasad, Sze Sing Lee, and Gayadhar Panda. "Reduced switch cascaded multilevel inverter with new selective harmonic elimination control for standalone renewable energy system." IEEE Transactions on Industry Applications 55.6 (2019): 7561-7574.
[30] Balakishan, Chouki, N. Sandeep, and M. V. Aware. "Design and Implementation of Three-Level DC-DC Converter with Golden Section Search Based MPPT for the Photovoltaic Applications." Advances in Power Electronics 2015 (2015).
[31] Kuncham, Sateesh Kumar, Kirubakaran Annamalai, and Nallamothu Subrahmanyam. "A two-stage t-type hybrid five-level transformerless inverter for PV applications." IEEE Transactions on Power Electronics 35.9 (2020): 9512-9523.
[32] Memon, Mudasir Ahmed, Marif Daula Siddique, Mekhilef Saad, and Marizan Mubin. "Asynchronous Particle Swarm Optimization-Genetic Algorithm (APSO-GA) based Selective Harmonic Elimination in a Cascaded H-Bridge Multilevel Inverter." IEEE Transactions on Industrial Electronics (2021).
[33] Siddique, Marif Daula, Mahajan Sagar Bhaskar, Muhyaddin Rawa, Saad Mekhilef, Mudasir Ahmed Memon, Sanjeevikumar Padmanaban, Dhafer J. Almakhles, and Umashankar Subramaniam. "Single-phase hybrid multilevel inverter topology with low switching frequency modulation techniques for lower order harmonic elimination." *IET Power Electronics* 13, no. 17 (2021): 4117-4127.
[34] Siddique, Marif Daula, Saad Mekhilef, Sanjeevikumar Padmanaban, Mudasir Ahmed Memon, and Chandan Kumar. "Single phase step-up switched-capacitor based multilevel inverter topology with SHEPWM." *IEEE Transactions on Industry Applications* (2020).

Sanjeevikumar Padmanaban (Member'12–Senior Member'15, IEEE) received the Ph.D. degree in electrical engineering from the University of Bologna, Bologna, Italy, in 2012 He was an Associate Professor at VIT University from 2012 to 2013. In 2013, he joined the National Institute of Technology, India, as a Faculty Member. In 2014, he was invited as a Visiting Researcher at the Department of Electrical Engineering, Qatar University, Doha, Qatar, funded by the Qatar National Research Foundation (Government of Qatar). He continued his research activities with the Dublin Institute of Technology, Dublin, Ireland, in 2014. Further, he served as an Associate Professor with the Department of Electrical and Electronics Engineering, University of Johannesburg, Johannesburg, South Africa, from 2016 to 2018. Since 2018, he has been a Faculty Member with the Department of Energy Technology, Aalborg University, Esbjerg, Denmark. He has authored over 300 scientific papers.

S. Padmanaban was the recipient of the Best Paper cum Most Excellence Research Paper Award from IET-SEISCON'13, IET-CEAT'16, IEEE-EECSI'19, IEEE-CENCON'19 and five best paper awards from ETAEERE'16 sponsored Lecture Notes in Electrical Engineering, Springer book. He is a Fellow of the Institution of Engineers, India, the Institution of Electronics and Telecommunication Engineers, India, and the Institution of Engineering and Technology, U.K. He is an Editor/Associate Editor/Editorial Board for refereed journals, in particular the IEEE SYSTEMS JOURNAL, IEEE Transaction on Industry Applications, IEEE ACCESS, *IET Power Electronics*, *IET Electronics Letters,* and Wiley-*International Transactions on Electrical Energy Systems,* Subject Editorial Board Member – *Energy Sources – Energies Journal*, MDPI, and the Subject Editor for the *IET Renewable Power Generation*, *IET Generation, Transmission and Distribution*, and *FACTS* journal (Canada).

Dhanamjayulu C (Member, IEEE) received the B.Tech. degree in electronics and communication engineering from JNTU University, Hyderabad, India, the M.Tech. degree in control and instrumentation systems from Indian Institute of Technology Madras, Chennai, India, and the Ph.D. degree in Power Electronics from the Vellore Institute of Technology, Vellore, India. He was a Postdoctoral Fellow with the Department of Energy Technology, Aalborg University, Esbjerg, Denmark from 2019 to January 2021. He is currently a Faculty Member and a member of the Control and Automation Department, School of Electrical Engineering, Vellore Institute of Technology. He is also a Senior Assistant Professor with the School of Electrical Engineering, Vellore Institute of Technology. Since 2010, he has been a Senior Assistant Professor with the Vellore Institute of Technology. He was invited as a Visiting Researcher with the Department of Energy Technology, Aalborg University, Esbjerg, Denmark, funded by the Danida Mobility Grant, Ministry of Foreign Affairs of Denmark on Denmark's International Development Cooperation. His research interests include multilevel inverters, power converters, active power filters, power quality, grid-connected systems, smart grid, electric vehicle, electric spring, and tuning of memory elements & controller parameters using soft-switching techniques for power converters, average modeling, steady-state modeling, small-signal modeling stability analysis of the converters and inverters.

Baseem Khan (Member, IEEE) received the B.Eng. degree in electrical engineering from Rajiv Gandhi Technological University, Bhopal, India in 2008, and the M.Tech and D.Phil. degrees in electrical engineering from the Maulana Azad National Institute of Technology, Bhopal, India, in 2010 and 2014, respectively. He is currently working as a Faculty Member at Hawassa University, Ethiopia. His research interest includes power system restructuring, power system planning, smart grid technologies, meta-heuristic optimization techniques, reliability analysis of renewable energy systems, power quality analysis, and renewable energy integration.